

Study the Effect of Lens Monochromatic Aberrations on Satellite Images Quality

Eng. Mohamed Ahmed Ali* Dr. Fawzy Eltohamy* Dr.Mohamed abdelhady * Dr. Gouda I. Salama*

*Department of Aircraft Electric Equipment, Military Technical College, Cairo, Egypt

Abstract - Satellite imaging is used for gathering detailed information about earth. However, there are many distortions associated with images taken by satellites optical sensors which degraded the image quality. A convenient measure of the image quality is the ability of the optical system to transfer various levels of details from object space to image plane. However the light diffraction and optical aberrations are main sources of image quality degradation.

This paper investigates the effect of different optical aberrations on satellite image quality. Also a comparative study among different types of aberrations is carried out. The imaging system (e.g. focal length, pixel size of the CCD, F-number, entrance aperture diameter, etc.) is simulated using MATLAB program. The optical aberrations are simulated by Zernike polynomial to determine their effects on the image quality. The presented algorithm (imaging system simulation) is applied on two high resolution remote sensing images, acquired by GeoEye-1 and IKONOS-1 satellites in order to study the effect of aberrations on the satellite images quality in terms of point spread function (PSF) and the modulation transfer function (MTF) variations. The evaluation of the quality of aberrated images is conducted with the help of the two widely used metrics: Mean Square Error (MSE) and Peak-Signal to Noise Ratio (PSNR).

Key Words: Optical aberrations, PSF, MTF, Zernike Polynomial, PSNR, and MSE.

1. INTRODUCTION

An optical aberration can be described in terms of the deviation of the deformed wave front from the ideal one at various distances from the optical axis. In fig (1), at the location of point B, the wave aberration is given by the distance AB, or it can be considered simply an imperfection in the way a lens focuses light. There are a number of different classifications of optical aberrations, and they affect sharpness, colour, focus, magnification, and distortion in satellite imaging [1].

To understand the impact of aberrations, the optical system, can be characterized by way of the point spread function PSF. The point spread function describes the optical system response, and also modulation transfer function MTF describes the image quality in classical optical systems (linear systems). The MTF is a graphical representation of

image quality that eliminates the need for decision-making by the observer [2].

The combined effect of the different parts of an optical system is determined by the convolution of the point spread functions (PSF). The point spread function of a diffraction limited lens is simply a disc, the image function is the convolution of the object function and the point spread function [3].

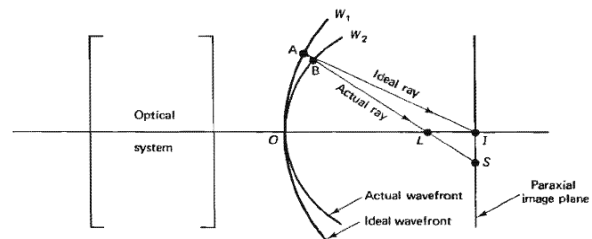


Fig -1: illustration of wave front aberration [2]

The normalized modulus of the two-dimensional Fourier transform of the overall PSF gives the total MTF which is a metric that describes how the spectral components of the target are affected by the optical properties of the propagation medium and the imaging system, [3]:

$$MTF(u, v) = \frac{\left| \iint_{-\infty}^{\infty} PSF(x, y) \times \exp[-2j2\pi(xu + yv)] dx dy \right|}{\iint_{-\infty}^{\infty} PSF(x, y) dx dy} \quad \text{eq. (1)}$$

Where x and y [m] are the spatial coordinates at the image plane, and u and v [cycle / rad.] are spatial frequency coordinates in the x and y directions, respectively, where $u = x/\lambda$ and $v = y/\lambda$ [rad-1].

In the other hand the Zernike polynomials are used to describe the aberrated wavefront in the pupil of an optical system. In general, the function describing an arbitrary wavefront in polar coordinates (ρ, θ) denoted by $W(\rho, \theta)$, can be expanded in terms of a sequence of polynomials Z that are orthonormal over the entire surface of the circular pupil as shown in figure (2), [4]:

$$W(\rho, \theta) = \sum C_n m Z_n^m(\rho, \theta) \quad \text{eq. (2)}$$

Where: C denotes the Zernike amplitudes or coefficients and Z the polynomials. The coordinate system is shown in figure (3). [5]

The advantage of expressing the wavefront by a linear combination of orthogonal polynomials is that the wavefront deviation represented by each term is a best fit (minimum fit variance) with respect to the actual wavefront. Then, any combination of these terms must also be a best fit [4]. One of the main advantages of the Zernike polynomials is their ability to describe arbitrary wavefronts or wave aberrations without any constraints to symmetry. This property is necessary, for instance, to describe the results of interferometric measurements [6].

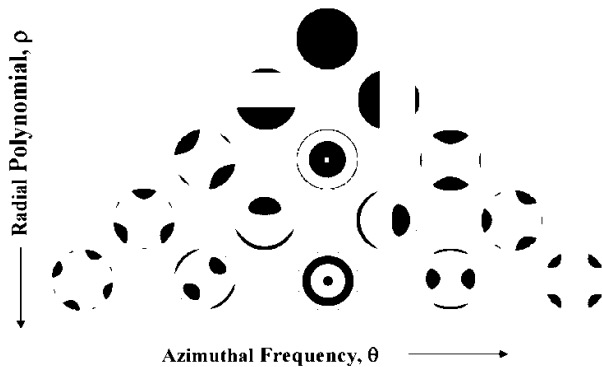


Fig -2: Zernike polynomial [5]

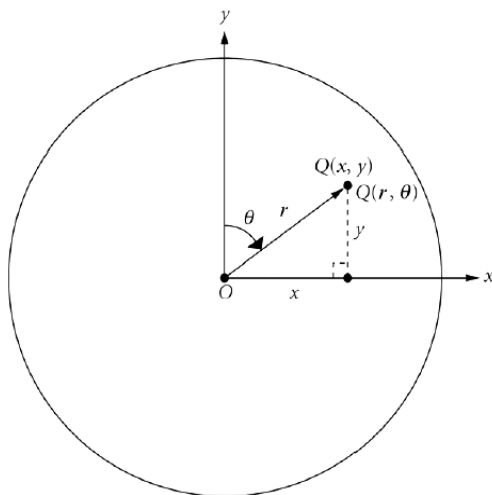


Fig -3: Cartesian (x,y) and polar (r,θ) coordinates of a point Q in the plane of a unit circle representing the circular exit pupil of an imaging system[5]

2. Types of monochromatic aberration

The monochromatic aberrations can be defined as outnumbering of the chromatic aberrations [7]. These aberrations may be due to incomplete optical design, manufacturing faults on the lens surfaces, inhomogeneities in the glass, or even decentring of the mechanical lens holders [8]. Different types of monochromatic aberrations are spherical, Coma, and Astigmatism, fig (4) [8].

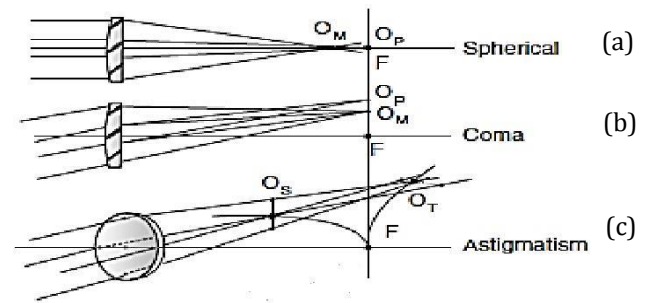


Fig -4: The primary optical aberrations shown for a lens [8]

Spherical aberration occurs when rays from a source at infinity on the optical axis do not converge at the same point; fig (4a) [9]. Coma makes the image projection blurred to the form of a comet. It is given in fig (4b) where the paraxial (central) rays do not have the same focus point as the marginal rays (edges of lens). Another occurrence is when the secondary mirror axis is misaligned with the primary mirror axis [9].

Astigmatism is when the incoming rays' point of focus is at different distances from the lens or mirror in the horizontal and vertical plane. It is simply an image blurring due to varying lens curvatures in different planes, fig (4c) [9].

Defocus and Trefoil are other types of optical aberrations. Defocus is a first order aberration and will vary as the distance to the center of the lens varies. Defocusing of the lens will cause the image to blow up in a blur or distort smaller and smaller, depending on whether it is inside focus or outside focus. This is easily fixed by moving the lens along its center axis until the image sharpens [10]. Trefoil resulting from surface deformation increases with the third power of field angle. Since its average axial value is not significantly lower than that of 3rd order coma, it would quickly become the dominant field aberration [11].

3. Quality Assessment of the aberrated images

The quality of the aberrated images is evaluated using the following two metrics:

- Root mean square error (RMSE)

It is the square root of the mean square error between the original and aberrated image. It detects the difference between the aberrated and the original image [12].

$$RMSE = \sqrt{\frac{1}{M \times N} \sum_{x=0}^{M-1} \sum_{y=0}^{N-1} (g(x, y) - f(x, y))^2} \quad \text{eq. (3)}$$

Where, $f(x,y)$ is the original or input image, $g(x,y)$ is the output image (the aberrated image) and $(M \times N)$ is The image size.

- Peak signal to noise ratio (PSNR)

Peak signal to noise ratio in (dB) is defined as [12, 13]:

$$PSNR = 10 \log \left[\frac{X_{\max}^2}{\frac{1}{M \times N} \sum_{x=0}^{M-1} \sum_{y=0}^{N-1} (g(x, y) - f(x, y))^2} \right] \quad \text{eq. (4)}$$

Where, X_{\max} is the maximum gray level (255 for 8-bit level) of the given input image. The PSNR is more commonly used than the RMSE, because people tend to associate the quality of an image with a certain range of PSNR. [12]

4. Experimental Work & Results Evaluation

To study the effects of optical aberrations on satellite imaging the following algorithm, illustrated in fig (5), is proposed.

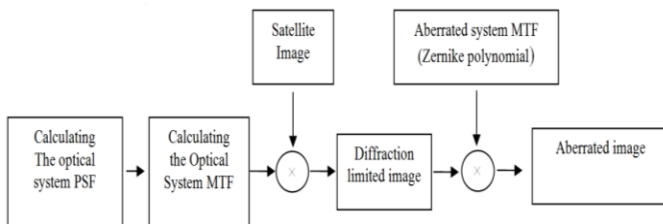


Fig -5: the proposed system algorithm

Two different satellite images, Image-1 and Image-2, fig (6) are used to study the optical aberrations effects. Image-1 and Image-2 are acquired by GeoEye-1 and Ikonos-1 satellites respectively. Table (1) gives the characteristics of the two images [14].

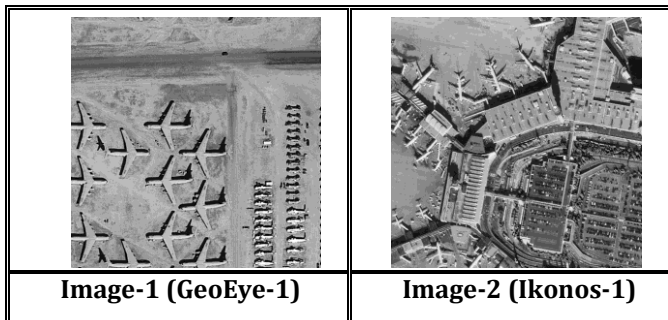


Fig -6: Tested set of images

Table -1: Characteristics of test set images

Image No.	Band (μm)	Resolution n (m)	Image area	Sample size (pixels)
Image-1 (GeoEye-1)	Panchromatic (0, 45 - 0, 8)	0.5	Arizona, (USA)	512 x 512
Image-2 (Ikonos-1)	Panchromatic (0, 45 - 0, 8)	1	Vancouver (Canada)	512 x 512

The proposed system which is illustrated in figure (5) was implemented using (MATLAB R2010b, 7.11.0) according to the following steps:

Step-1, Calculating and constructing the PSF curve of the diffraction-limited system in terms of ($\lambda F\#$). The intensity of the Airy diffraction pattern of a circular aperture is given by the squared modulus of the Fourier transform of the circular aperture [15]:

$$I(\theta) = I_0 \left(\frac{2J_1(ka \sin\theta)}{ka \sin\theta} \right)^2 = I_0 \left(\frac{2J_1(x)}{x} \right)^2 \quad \text{eq. (5)}$$

where I_0 is the maximum intensity of the pattern at the Airy disc center, J_1 is the Bessel function of the first kind of order one, $k = 2\pi/\lambda$ is the wave number [dimensionless], a is the radius of the aperture [m], and θ is the angle of observation [rad], i.e. the angle between the axis of the circular aperture and the line between aperture center and observation point [15].

Step-2, studying the resulting PSF due to various types of monochromatic aberrations, which include astigmatism, spherical, coma, trefoil and defocus, using equation (2) to get the aberrated pattern then applying the Bessel function to obtain the aberrated PSF pattern as shown in figure (8).

Step-3, comparing the obtained MTF curves at fixed aperture diameter of 0.5 [m] for the two satellite images using equation (1).

Step-4, calculating the Mean Square Error (MSE) and Peak Signal-to-Noise Ratio (PSNR) for the different aberration types for the two satellite images.

In step 1, the assumed optical system parameters are: wavelength (λ) = 0.55 [μm], focal number ($F\#$) = 1, detector pixel size = 9 [μm], and aperture diameter (D) = 0.5 [m].

Figure (7) shows the diffraction-limited system PSF. The first zero of the normalized radius of the first minima will be located at $r = 1.22 \lambda F\#$, where λ is the wavelength and $F\#$ is the focal number ($F\# = f / D$)

Various monochromatic aberrations are modeled using Zernike polynomial by changing Zernike polynomial coefficients (m and n) as given in table (2), [6].

Table -2: Zernike polynomial and aberration type [6]

Aberration type	m	n
Defocus	0	2
Spherical	0	4
Coma	1	3
Astigmatism	2	2
Trefoil	3	-3

In step-2, the PSF of the diffraction limited system is compared with the other PSF curves of different aberrations types. From this comparison, figure (8), we conclude the following:

- For a diffraction-limited imaging system, about 84% of the collected flux is concentrated in an Airy disc of radius $r = 1.22 \lambda F\#$ [m].
- For the different types of monochromatic aberrations, the Airy pattern is deformed due to the effect of the various aberrated PSFs.

In step-3, A comparison of the MTF curves, at fixed aperture diameter, 0.5 [m], of the two aberrated satellite images, by different aberrations, with the diffraction-limited MTF curve is conducted. From fig (9) and (10) we can conclude the following:

- In the case of a diffraction-limited imaging system, the resulting image is very close to the original image.
- The MTF curves for both Coma and Spherical aberrations are significantly different from the case of the diffraction-limited curve which in turn leads to produce degraded images.

Finally Mean Square Error and Peak Signal-to-Noise Ratio metrics of the degraded images are used to evaluate the effect of the applied monochromatic aberrations on the quality of the resulting images, at aperture diameter: $D = 0.5$ [m]. Table (3) illustrates the results of applying the mentioned metrics on the two satellite images.

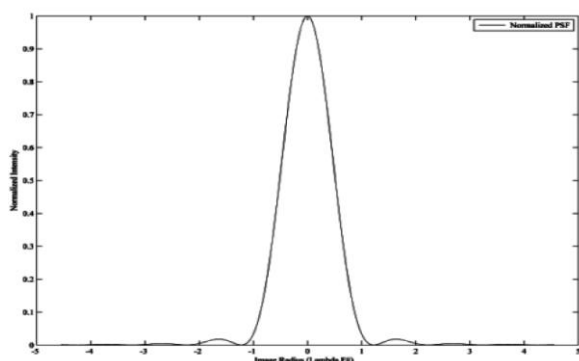


Fig -7: The system Normalized Point Spread Function curve

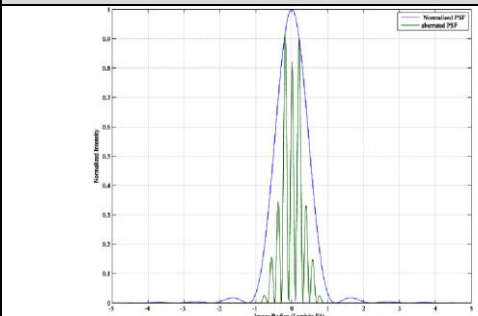
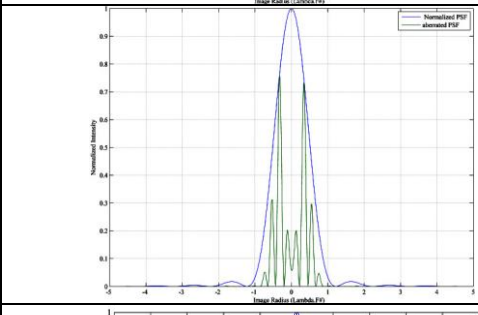
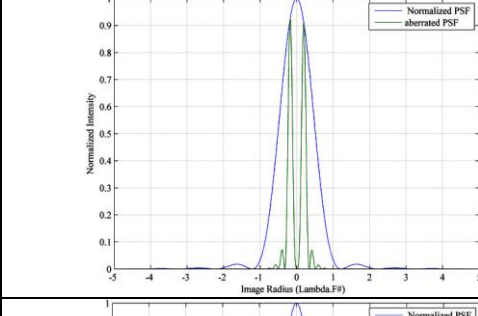
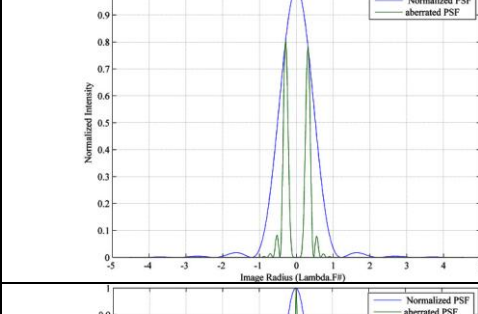
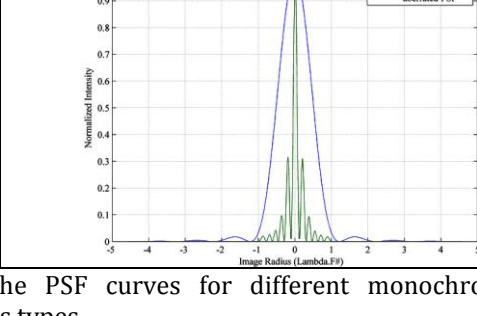
Aberration type	Corresponding PSF curve with respect to diffraction limited PSF
Astigmatism	
Coma	
Defocus	
Spherical aberration	
Trefoil	

Fig -8: The PSF curves for different monochromatic aberrations types

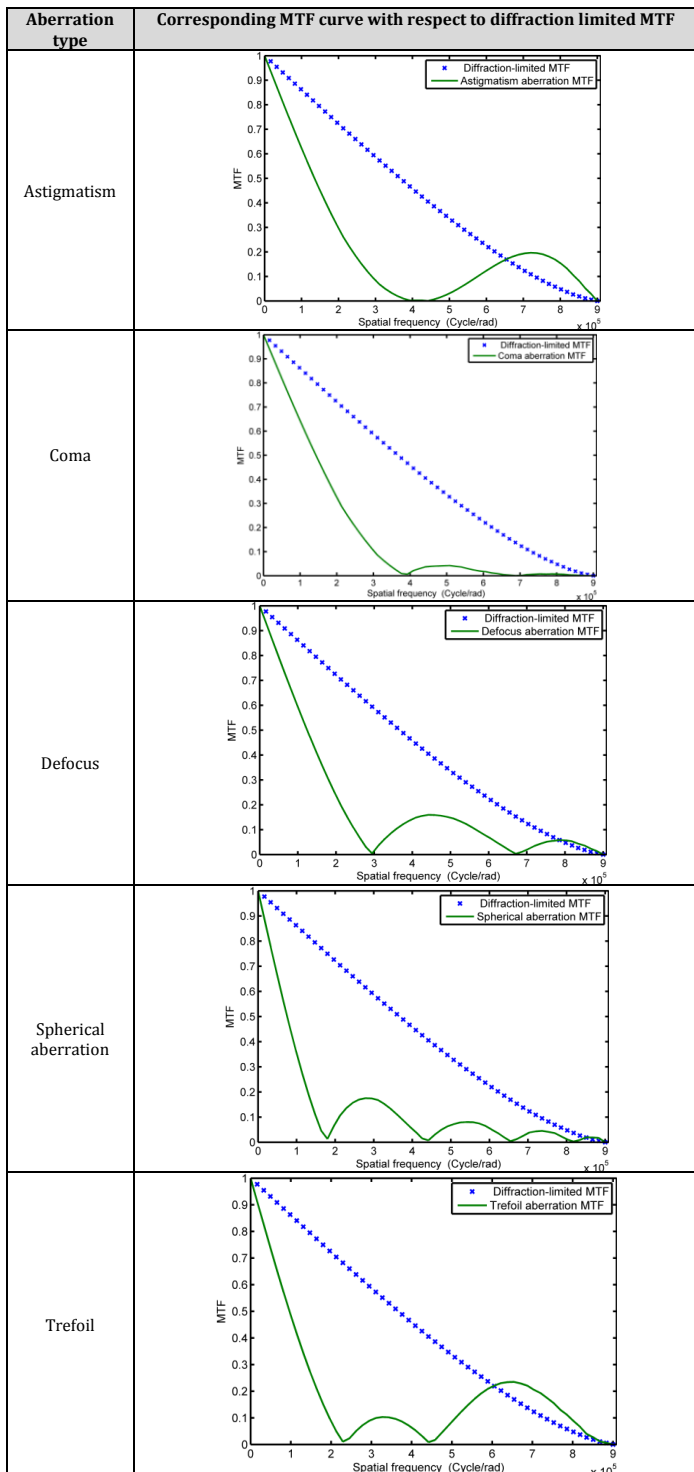


Fig -9: The MTF curves for different aberration types

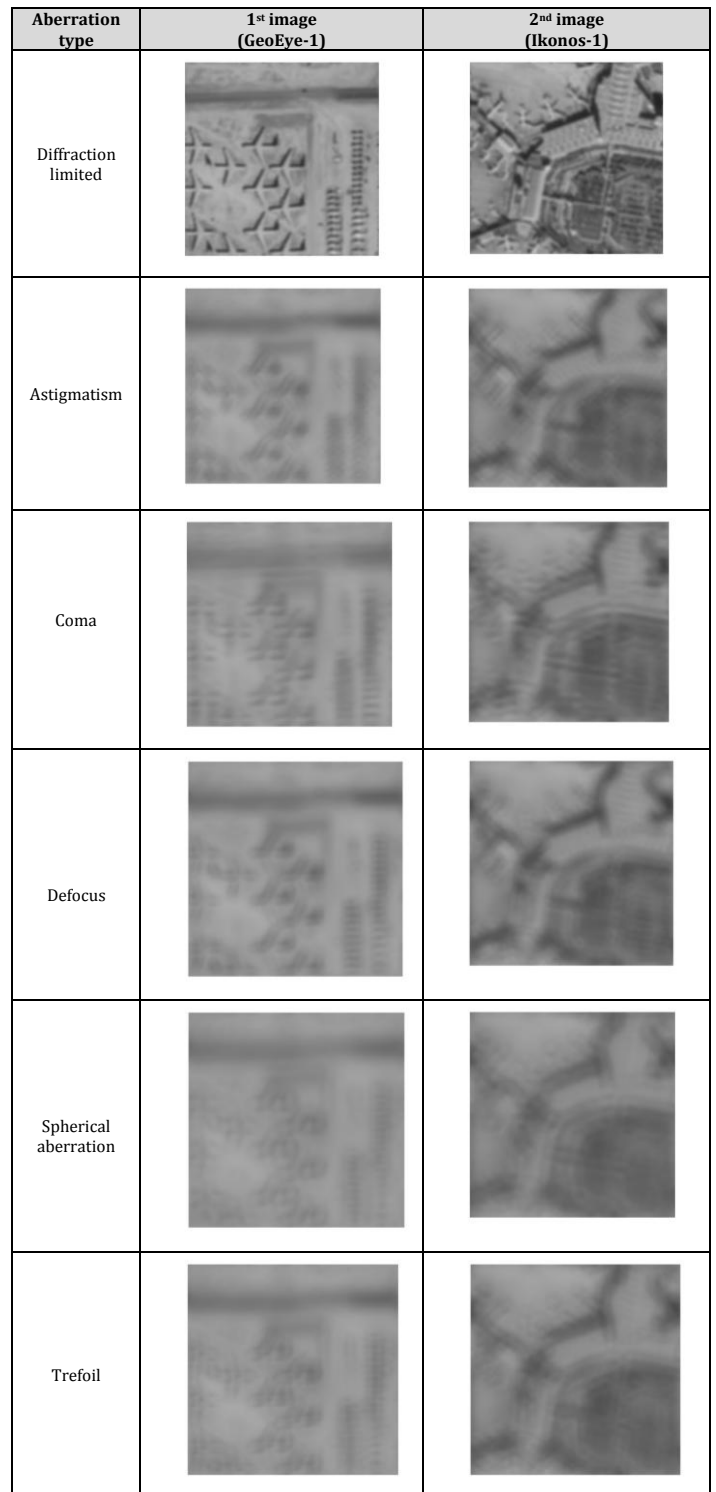


Fig -10: Degraded satellite images due to various types of monochromatic aberration.

Table -3: Peak Signal-to-Noise Ratio (PSNR) and mean square error (MSE) for image (1)

Image no.	Quality metrics	Diffraction limited	Astigmatism	Defocus	Trefoil	Coma	Spherical
Image (1)	PSNR	20.5781	18.4985	18.405	18.242	18.17	18.100
	RMSE	569.209	918.824	938.63	974.58	989.7	1007
Image (2)	PSNR	19.5486	17.4485	17.438	17.152	17.05	16.969
	RMSE	721.475	1170.1	1172.7	1252.6	1282	1306.7

Table (3) shows that:

- In case of diffraction-limited imaging system, the resulting images give the best results of PSNR and RMSE in comparison with the result due to the different types of monochromatic aberrations.
- The spherical aberration gives the lowest PSNR values for both images, also gives the highest RMSE values, indicating the severe degrading effect of spherical aberration in comparison with other types of monochromatic aberrations.

5. CONCLUSIONS

From figures (8, 9 and 10) and table (3) we can conclude that:

- In the absence of optical aberrations, the image quality of an optical system is limited by diffraction, which is the subtle bending or spreading of light at the edge of an aperture.
- The spherical aberration is the most worth aberration effect for the all types of aberrations which indicates the worst image quality. [9]
- The Astigmatism aberration gives (numerically) values in (PSNR, RMSE) closer to the values obtained by (Diffraction limited) system while (coma & Spherical) aberration are largely different.
- Aberrations are reduced to a minimum by shaping the lenses in an appropriate manner and choosing appropriate types of glass. Differences in dispersion between various types of glass are used to make corrections in color, or achromatisation.[8]

REFERENCES

[1] Frank L-Pedrotti, Leno S. Pedrotti "Introduction to Optics" Prentice-Hall International, Inc, second edition 1993.
 [2] Franziska S. Frey, James M. Reilly "Digital Imaging for Photographic Collections -Foundations for Technical

Standards" Image Permanence Institute Rochester Institute of Technology, 2006
 [3] Mohamed E. Hanafy, Michael C. RoggemannK, Durdu O. Guney "Reconstruction of images degraded by aerosol scattering and measurement noise" (SPIE) [DOI: 10.1117/1.OE.54.3.033101].
 [4] Larry N. Thibos, PhD; Raymond A. Applegate, OD, PhD; James T. Schwiegerling "Standards for Reporting the Optical Aberrations of Eyes" Journal of Refractive Surgery Volume 18 September/October 2002
 [5] Guenther, Robert D. "Modern Optics" John Wiley & Sons, Inc., 1990.
 [6] Herbert Gross, Henriette muller,Brand dorband "Handbook of Optical Systems" Vol. 3. Aberration Theory and Correction of Optical Systems. Copyright © 2007 WILEY-VCH Verlag GmbH & Co. ISBN: 978-3-527-40379-0
 [7] Kjell J. Gåsvik "Optical Metrology Third Edition" John Wiley & Sons Ltd, 2002 ISBN 0-470-84300-4.
 [8] Rainer Sandau "Digital Airborne Camera : Introduction and Technology" Springer Dordrecht Heidelberg London New York 2010 [DOI: 10.1007/978-1-4020-8878-0]
 [9] Daniel Pettersson "Optical Design and Tomographic Retrievals for the MATS Satellite Mission" Master of Science in Engineering Technology Space Engineering Luleå University of Technology , 2015
 [10] Daniel Malacara and Zacarias Malacara "Handbook of Optical Design: Second Edition" by Marcel Dekker, Inc.2004
 [11] Vasudevan Lakshminarayanan and Andre Fleck "Tutorial Review Zernike Polynomials: a guide" Journal of Modern Optics,2011
 [12] AL Bovik, "Hand book of Image and Video Processing", Department of Electrical and Computer Engineering, The University of Texas at Austin, 2000
 [13] M. Mrak, S. Grgić, M. Grgić. Picture Quality Measures in Image Compression Systems. In Proceedings of the Eurocon 2003 conference, p. 233-237, Ljubljana, Slovenia 2003
 [14] Data sheets from <http://www.digitalglobe.com> and <http://www.spotimage.com>
 [15] S. wong and R. jassemi- Zargani, "predicting image quality of servillance sensors" Defence Research and Development ,Canada (DRDC), DRDC – RDDC – 2014 – 2014 – R97 , October 2014.